Supporting Information to:

Chemical analysis of Chang'e-5 lunar soil using LA–ICP–MS in highly diluted fused glass discs

Shitou Wu[1, 2, *], Dingshuai Xue[1, 2], Yueheng Yang[1, 2], Hao Wang[1, 2], Chunlai Li[3] and Fuyuan Wu[1, 2]

1. State Key Laboratory of Lithospheric and Environmental Coevolution, Institute of Geology and Geophysics, Chinese Academy of Sciences, Beijing, 100029, P.R. China
2. College of Earth and Planetary Science, University of Chinese Academy of Sciences, Beijing, 100049, P.R. China
3. Key Laboratory of Lunar and Deep Space Exploration, National Astronomical Observatories, Chinese Academy of Sciences, 100101, Beijing, P.R. China

Corresponding author E-mail address: shitou.wu@mail.iggcas.ac.cn;

This supporting information material includes the detail sample information, the preparation of highly diluted fused glass discs, and the LA–ICP–MS analysis. Table S1-S4 and Figure S1-S5 and the reference list were listed in this material as well.

Sample information.

The CE-5 lunar sample analyzed is CE5C0800YJFM002 obtained from China's CE-5 mission to the mid-latitude region in the northeastern Oceanus Procellarum on the Moon. The physical and chemical properties have been reported in previous studies[1-5]. The CE-5 lunar samples are composed mostly of basalt, impact glass, agglutinates, and mineral fragments. The basalts can be classified as low-Ti and highly fractionated based on their TiO_2 contents (~5.3 wt.%) and Mg# (~28), and have an age of 2030 ± 4 Ma[2, 5, 6]. A total of 30 mg of the sample was weighed accurately for LA–ICP–MS analysis. Two certified basaltic standards produced by the United States Geological Survey (BCR-2 and BHVO-1) were used for quality control. The recommended values of these two standards were taken from GeoReM (Version 35; http://georem.mpch-mainz.gwdg.de/).[7]

Preparation of highly diluted fused glass discs (flux:sample = 100:1). Pre-mixed anhydrous lithium borate powder (67% lithium tetraborate, 33% lithium metaborate; Claisse, Quebec, Canada) was used as flux to prepare the glass discs. Ammonium bromide (≥99.0%, ACS reagent) was purchased from Sinopharm Chemical Reagent Company (Shanghai, China) as an exfoliation agent. The sample powder and flux were dried in an oven at 110 °C for 24 hours. The dried samples and flux were then cooled to room temperature and placed in a glass desiccator before being weighted. Flux (3000.0 ± 0.2 mg) and sample (30.0 ± 0.1 mg) powders were weighed in sequence into a Pt–Au crucible. The flux and sample were mixed well using a glass rod and 0.15 mL aqueous ammonium bromide solution (0.12 g mL^{-1}) was added as an exfoliation agent. The glass discs were prepared following Xue et al. [8] (Program 3 of the M4 automatic fluxer). Due to the small sample size, the discs needed to be prepared by hand during the final stage of the fusion cycle (Figure 1). The major-element composition of the fused CE-5 glass disc was previously analyzed by X-ray fluorescence spectrometer (XRF) [1].

LA–ICP–MS analysis. Elemental abundances in the fused glass discs were determined by LA–ICP–MS using an Element XR high-resolution ICP–MS instrument (Thermo Fisher Scientific, USA) coupled to a 193 nm ArF excimer laser system (GeoLas HD, Lambda Physik, Göttingen, Germany) at the State Key Laboratory of Lithospheric and Environmental Coevolution, Institute of Geology and Geophysics, Chinese Academy of Sciences, Beijing, China. The approach was similar to that outlined by Wu et al. [9], with isotopes measured using peak-hopping mode. The instrument parameters are listed

in Table S1. To improve the instrument sensitivity, a modified Jet sample cone (orifice diameter enlarge from 1.1 mm to 1.2 mm) were used. Helium was used as the ablation gas to improve the transport efficiency for the ablated aerosols. ARM-2 reference glass was used for external calibration[9, 10] and highly diluted fused BCR-2 and BHVO-1 glass discs were used for quality control. To further simplification of the quantification procedure, we used the bulk normalization strategy based on Li_2O, B_2O_3, SiO_2, TiO_2, Al_2O_3, FeO, MnO, MgO, CaO, K_2O, and P_2O_5 as 100 wt% for data processing. With this approach, it is not required for a known internal standard (e.g., Si and Ca) for standardization. The data were reduced d using Iolite software [11] with an in house built DRS [12].

Table S1 Typical LA–SF–ICP–MS instrumental conditions.

Laser ablation system	
Make, model, and type	Coherent, GeoLas HD
Ablation cell	In-house cell, aerosol dispersion volume <3 cm^3
Laser wavelength	193 nm
Pulse duration	20 ns
Energy density	8.0 J cm^{-2}
Repetition rate	10 Hz
Spot size	90 μm
Sampling mode	Single hole drilling, with two cleaning pulses
Ablation gas flow	0.75 L min^{-1} (He)
Ablation duration	50s
ICP–MS instrument	
Make, model, and type	Thermo Fisher Scientific Element XR
Radio frequency power	1320 W
Guard electrode	Disconnected
Cone combinations	Standard sampler + H version skimmer (Nickel)
Fore vacuum P (mbar)	1.8×10^{-3} (S + H)
High vacuum P (mbar)	2.0×10^{-7} (S + H)
Coolant gas flow (Ar)	15.00 l min^{-1}
Auxiliary gas flow (Ar)	0.80 l min^{-1}
Carrier gas flow (Ar)	0.95 l min^{-1}
Scan mode	E-scan
Isotopes measured (dwell time)	^{7}Li (10 ms), ^{11}B (10 ms), ^{24}Mg (10 ms), ^{27}Al (10 ms), ^{30}Si (10 ms), ^{31}P (10 ms), ^{39}K (10 ms), ^{44}Ca (10 ms), ^{45}Sc (10 ms), ^{49}Ti (10 ms), ^{55}Mn (10 ms), ^{59}Co (10 ms), ^{60}Ni (10 ms), ^{71}Ga (10 ms), ^{85}Rb (10 ms), ^{88}Sr (10 ms), ^{89}Y (10 ms), ^{90}Zr (10 ms), ^{93}Nb (10 ms), ^{133}Cs (10 ms), ^{137}Ba (10 ms), ^{139}La (10 ms), ^{140}Ce (10 ms), ^{141}Pr (10 ms), ^{146}Nd (10 ms), ^{147}Sm (10 ms), ^{153}Eu (10 ms), ^{158}Gd (10 ms), ^{159}Gd (10 ms), ^{163}Tb (10 ms), ^{165}Ho (10 ms), ^{166}Er (10 ms), ^{169}Tm (10 ms), ^{173}Yb (10 ms), ^{175}Lu (10 ms), ^{177}Hf (10 ms), ^{181}Ta (10 ms), ^{208}Pb (10 ms), ^{232}Th (10 ms), ^{238}U (10 ms)
Mass window	20%
Samples per peak	20
Detection system	Single secondary electron multiplier in triple mode, ion counter, analogue, and Faraday cups
Resolution	$m/\Delta m = 300$
Total integration time per reading	0.38 s

Table S2 The potential Li-, B-, O-, and Ar-based polyatomic interferences on the targeted isotopes

□ □ □ □	Li, B, O and Ar based polyatomic ions		Flux reagent impurities
	Monovalent ions	Divalent ions	
^{24}Mg		$^{10}B^{38}Ar^{2+}$	Amount
^{27}Al	$^{11}B^{16}O^{+}$		Amount
^{29}Si	$^{11}B^{18}O^{+}$		Amount
^{30}Si			Amount
^{31}P			Significant
^{39}K			Limited
^{43}Ca	$^{7}Li^{36}Ar^{+}$		Amount
^{44}Ca			Amount
^{45}Sc	$^{7}Li^{38}Ar^{+}$		Limited
^{47}Ti	$^{7}Li^{40}Ar^{+}$, $^{11}B^{36}Ar^{+}$		Limited
^{49}Ti	$^{11}B^{38}Ar^{+}$, $^{11}B^{40}Ar^{+}$		Limited
^{57}Fe			Limited
^{66}Zn	$^{10}B^{16}O^{40}Ar^{+}$		Limited
^{66}Zn			Limited
^{71}Ga			Amount
^{886}Sr			Amount
^{137}Ba			Amount
^{208}Pb			Amount

Table S3 The limit of detections (LODs) of 38 elements pf our technique were calculated based on the protocol by Pettke et al. (2012)[12]

Element	LODs (μg g^{-1})
K	76
Sc	3.6
Mn	14
Co	0.98
Ni	32
Ga	7.8
Rb	0.52
Sr	1.8
Y	0.21
Zr	3.3
Nb	0.37
Cs	0.16
Ba	1.1
La	0.12
Ce	0.09
Pr	0.09
Nd	0.33
Sm	0.51
Eu	0.18
Gd	0.19
Tb	0.11
Dy	0.16
Ho	0.08
Er	0.12
Tm	0.08
Yb	0.54
Lu	0.08
Hf	0.25
Ta	0.12
Pb	0.13
Th	0.18
U	0.03

Table S4 Trace element data of BCR-2 and BHVO-1. The reference values of these two materials were listed for comparison.

□	BCR-2				BHVO-1			
□	Ref.val.	2s	Mean	SD	Ref.val.	2s	Mean	SD
SiO_2	54.0	0.2	53.9	1.0	49.6	0.1	49.6	0.9
TiO_2	2.27	0.02	2.27	0.05	2.73	0.02	2.72	0.06
Al_2O_3	13.5	0.1	13.6	0.8	13.4	0.06	13.4	0.6
FeO	12.4	0.2	12.3	0.5	11.3	0.2	11.5	0.6
MnO	0.197	0.003	0.202	0.006	0.169	0.002	0.164	0.003
MgO	3.60	0.04	3.54	0.12	7.26	0.04	7.17	0.12
CaO	7.11	0.08	6.98	0.39	11.4	0.1	11.5	0.6
K_2O	1.77	0.02	1.72	0.06	0.513	0.004	0.529	0.008
P_2O_5	0.359	0.010	-	-	0.359	0.010	-	-
Sc	33.5	0.4	34.2	1.5	31.8	0.3	33.5	3.4
Co	37.3	0.4	40.3	2.1	44.9	0.3	43.7	3.7
Ni	12.57	0.3	11.7	2.0	120	1	111	14
Ga	22.1	0.2	20.7	1.4	21.3	0.2	22.2	3.9
Rb	46.0	0.5	38.8	3.3	9.26	0.10	8.04	1.04
Sr	337	7	363	7	394	2	406	7
Y	36.1	0.4	34.4	2.3	25.9	0.3	24.2	2.0
Zr	187	2	181	11	171	1	165	1
Nb	12.4	0.2	13.5	3.9	18.1	0.2	16.7	1.6
Cs	1.16	0.02	0.92	0.23	0.100	0.002	1.66	3.29
Ba	684	5	734	29	131	1	128	15
La	25.1	0.2	25.5	1.0	15.2	0.1	14.4	0.5
Ce	53.1	0.3	47.7	1.8	37.53	0.19	34.4	2.4
Pr	6.83	0.04	6.68	0.63	5.34	0.03	4.87	0.55
Nd	28.3	0.4	30.2	2.2	24.3	0.3	24.0	2.9
Sm	6.55	0.05	7.07	1.81	6.02	0.06	5.48	1.78
Eu	1.99	0.02	1.89	0.38	2.04	0.01	2.05	0.24
Gd	6.81	0.08	6.31	0.73	6.21	0.04	5.57	0.87
Tb	1.08	0.03	1.01	0.13	0.939	0.006	0.96	0.17
Dy	6.42	0.06	6.25	0.88	5.28	0.03	5.47	0.17
Ho	1.31	0.01	1.51	0.17	0.989	0.005	1.04	0.19
Er	3.67	0.04	3.95	0.61	2.51	0.01	2.36	0.38
Tm	0.534	0.006	0.54	0.21	0.335	0.003	0.330	0.140
Yb	3.39	0.04	3.18	1.04	1.99	0.03	1.59	0.61
Lu	0.505	0.008	0.400	0.060	0.275	0.002	0.390	0.090
Hf	4.97	0.03	5.67	0.48	4.47	0.03	4.65	1.25
Ta	0.785	0.018	0.750	0.110	1.15	0.02	1.38	0.36
Pb	10.6	0.2	13.7	2.3	1.65	0.04	1.73	0.3
Th	5.83	0.05	6.28	1.11	1.22	0.02	1.40	0.48
U	1.68	0.02	1.57	0.08	0.412	0.035	0.450	0.160

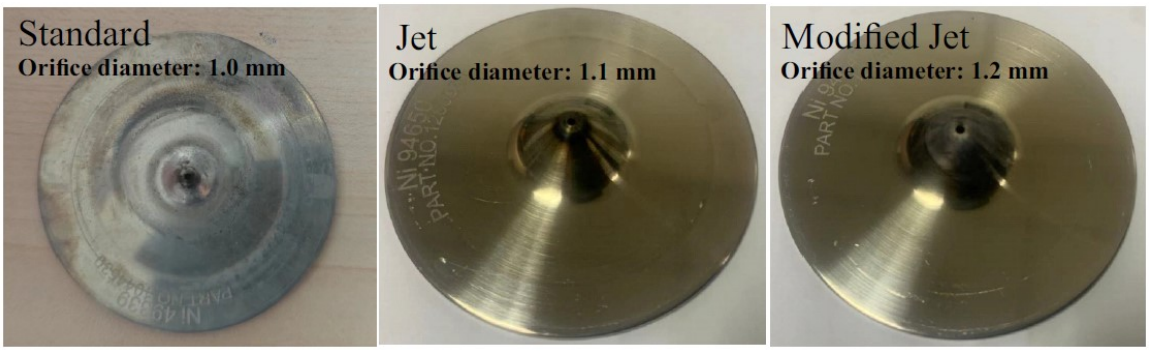

Figure S1 Exterior comparison of the Standard cone, Jet cone and modified Jet cones

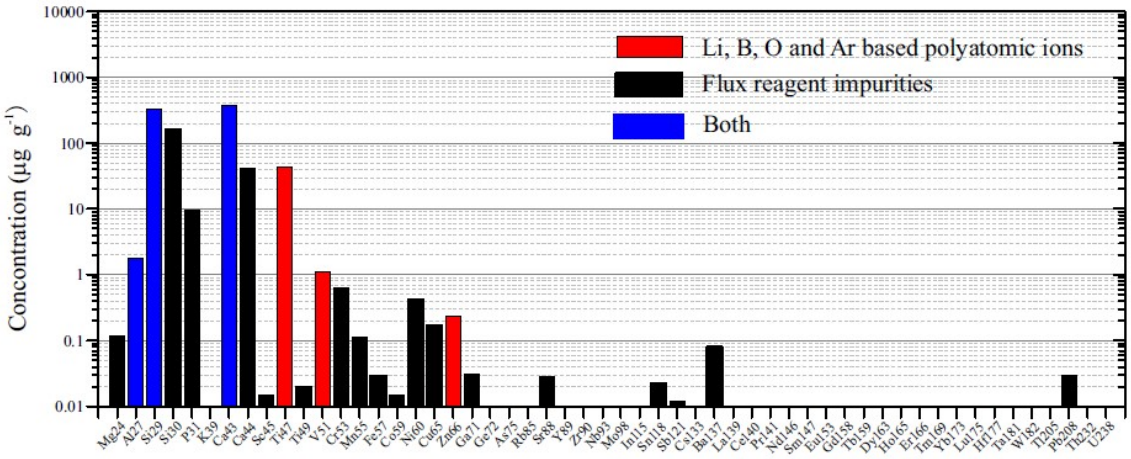

Figure S2 Identified interferences from lithium borate disks. The interferences were divided in two groups:(1) impurities in the reagent and contamination during preparation, and (2) Li-, B-, O-, and Ar-based polyatomic ions.

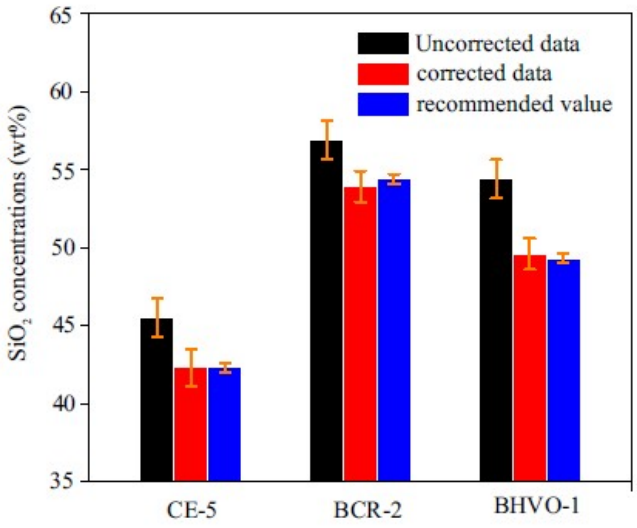

Figure S3. Comparison the interference-corrected and uncorrected SiO results of CE-5, BCR-2 and BHVO-1

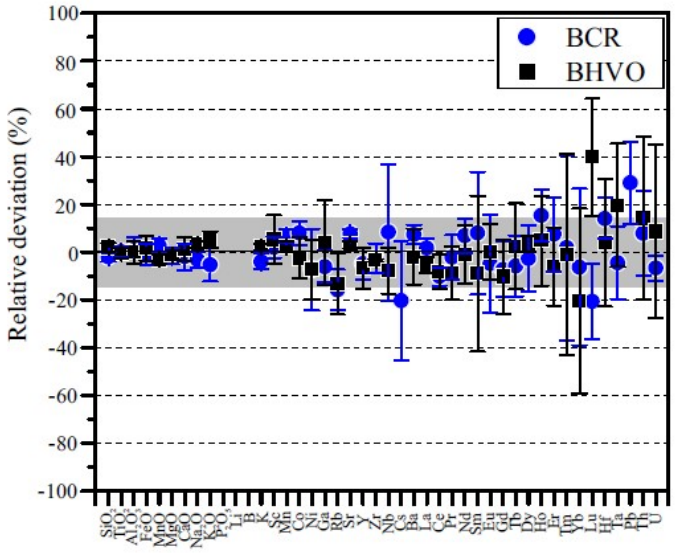

Figure S4. The analytical accuracy of BCR-2 and BHVO-1 glass disc. Relative deviations are given as 100 × (measured value − reference value)/reference value.

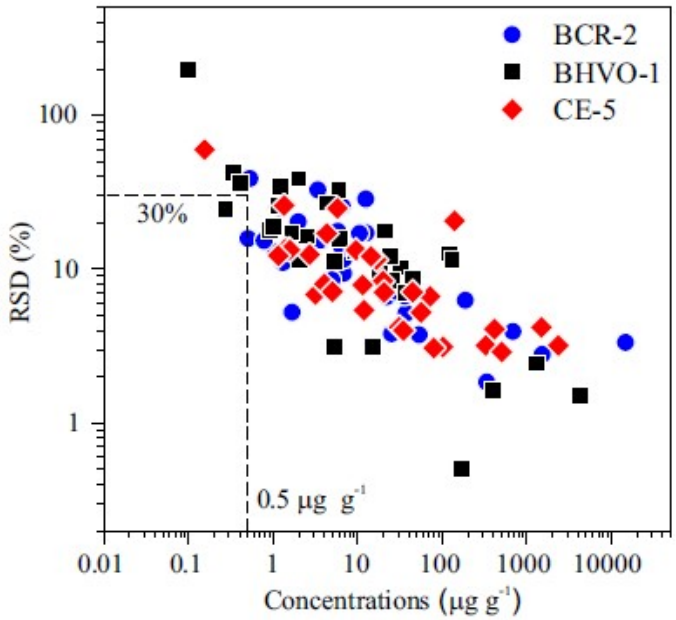

Figure S5. The analytical precision as function of elemental concentrations. The analytical precision is given as the relative standard deviation. There is a negative linear correlation between concentration and RSD on logarithmic plots

References

1. C. Li, H. Hu, M.-F. Yang, Z.-Y. Pei, Q. Zhou, X. Ren, B. Liu, D. Liu, X. Zeng, G. Zhang, H. Zhang, J. Liu, Q. Wang, X. Deng, C. Xiao, Y. Yao, D. Xue, W. Zuo, Y. Su, W. Wen and Z. Ouyang, *Nati. Scie, Revi.*, 2021, DOI: 10.1093/nsr/nwab188.
2. Q.-L. Li, Q. Zhou, Y. Liu, Z. Xiao, Y. Lin, J.-H. Li, H.-X. Ma, G.-Q. Tang, S. Guo, X. Tang, J.-Y. Yuan, J. Li, F.-Y. Wu, Z. Ouyang, C. Li and X.-H. Li, *Nature*, 2021, DOI: 10.1038/s41586-021-04100-2.
3. H.-C. Tian, H. Wang, Y. Chen, W. Yang, Q. Zhou, C. Zhang, H.-L. Lin, C. Huang, S.-T. Wu, L.-H. Jia, L. Xu, D. Zhang, X.-G. Li, R. Chang, Y.-H. Yang, L.-W. Xie, D.-P. Zhang, G.-L. Zhang, S.-H. Yang and F.-Y. Wu, *Nature*, 2021, DOI: 10.1038/s41586-021-04119-5.
4. S. Hu, H. He, J. Ji, Y. Lin, H. Hui, M. Anand, R. Tartèse, Y. Yan, J. Hao, R. Li, L. Gu, Q. Guo, H. He and Z. Ouyang, *Nature*, 2021, DOI: 10.1038/s41586-021-04107-9.
5. F.-Y. Wu, Q.-L. Li, Y. Chen, S. Hu, Z.-Y. Yue, Q. Zhou, H. Wang, W. Yang, H.-C. Tian, C. Zhang, J.-H. Li, L.-X. Li, H.-J. Hui, C.-L. Li, Y.-T. Lin, X.-H. Li and J. W. Delano, *Annual Review of Earth and Planetary Sciences*, 2024, DOI: https://doi.org/10.1146/annurev-earth-040722-100453.
6. X. Che, A. Nemchin, D. Liu, T. Long, C. Wang, M. D. Norman, K. H. Joy, R. Tartese, J. Head, B. Jolliff, J. F. Snape, C. R. Neal, M. J. Whitehouse, C. Crow, G. Benedix, F. Jourdan, Z. Yang, C. Yang, J. Liu, S. Xie, Z. Bao, R. Fan, D. Li, Z. Li and S. G. Webb, *Science*, 2021, **0**, eabl7957.
7. K. P. Jochum, U. Nohl, K. Herwig, E. Lammel, B. Stoll and A. W. Hofmann, *Geostand. Geoanal. Res.*, 2005, **29**, 333-338.
8. D.-S. Xue, B.-X. Su, D.-P. Zhang, Y.-H. Liu, J.-J. Guo, Q. Guo, J.-F. Sun and S.-Y. Zhang, *J. Anal. At. Spectrom.*, 2020, **35**, 2826-2833.
9. S. Wu, G. Wörner, K. P. Jochum, B. Stoll, K. Simon and A. Kronz, *Geostand. Geoanal. Res.*, 2019, **43**, 567-584.
10. S. Wu, Y. Yang, K. P. Jochum, R. L. Romer, J. Glodny, I. P. Savov, S. Agostini, J. C. M. De Hoog, S. T. M. Peters, A. Kronz, C. Zhang, Z. Bao, X. Wang, Y. Li, G. Tang, L. Feng, H. Yu, Z. Li, Z. Le, J. Lin, Y. Zeng, C. Xu, Y. Wang, Z. Cui, L. Deng, J. Xiao, Y. Liu, D. Xue, Z. Di, L. Jia, H. Wang, L. Xu, C. Huang, L. Xie, A. Pack, G. Wörner, M. He, C. Li, H. Yuan, F. Huang, Q. Li, J. Yang, X. Li and F. Wu, *Geostand. Geoanal. Res.*, 2021, **45**, 719-745.
11. C. Paton, J. Hellstrom, B. Paul, J. Woodhead andJ. Hergt. 2011. *J. Anal. At. Spectrom.*, 26(12), 2508-2518.
12 S. Wu, C. Huang, L. Xie, Y. Yang, and J. Yang. 2020. Chinese Journal of Analytical Chemistry, 46(10), 1628-1636..
13. T. Pettke, F. Oberli, A. Audétat, M. Guillong, A. C. Simon, J. J. Hanley and L. M. Klemm, *Ore Geol. Revi.*, 2012, **44**, 10-38.